HIGHER SCHOOL OF COMMUNICATION OF TUNIS

Multipath Propagation and Diversity

Analysis and Simulation of Vehicle-to-Vehicle Fading Channels

Prepared by:

Saif Iddin Gharbi
Mouhamed Amine Trabelsi
Amal Madhi
Sirine Charrada
Chiheb El Din El Zidi

INDP2F

Academic Year 2024-2025

Contents

1 Introduction

Vehicle-to-Vehicle (V2V) communications represent a crucial component of modern intelligent transportation systems. In V2V scenarios, the wireless channel exhibits unique characteristics due to the mobility of both transmitter and receiver. This study focuses on analyzing and simulating V2V multipath channels in Rayleigh fading environments.

2 Theoretical Analysis

2.1 Channel Power Gain Distribution

Starting from the complex channel gain expression:

$$h = h_1 h_2 = (x_1 + jy_1)(x_2 + jy_2) \tag{1}$$

The PDF of the envelope R = —h— is given by:

$$p_R(z) = \frac{4z}{\sigma_1^2 \sigma_2^2} K_0\left(\frac{2z}{\sigma_1 \sigma_2}\right) \tag{2}$$

For the channel power gain = R², using the transformation method:

$$p_\Omega(w) = p_R(\sqrt{w}) \left| \frac{d}{dw} \sqrt{w} \right| \tag{3}$$

This yields:

$$p_\Omega(w) = \frac{2}{\sigma_1^2 \sigma_2^2} K_0\left(\frac{2\sqrt{w}}{\sigma_1 \sigma_2}\right) \tag{4}$$

2.2 Signal-to-Noise Ratio Distribution

For an AWGN channel with noise power ² and transmit power P, the SNR is related to by:

$$\gamma = \frac{P^{tx} \Omega}{\sigma_n^2} \tag{5}$$

Using the transformation method with the change of variable = (P/²), we get:

$$p_\gamma(g) = \frac{\sigma_n^2}{P^{tx}} \cdot \frac{2}{\sigma_1^2 \sigma_2^2} K_0\left(\frac{2\sqrt{g\sigma_n^2 / P^{tx}}}{\sigma_1 \sigma_2}\right) \tag{6}$$

3 Simulation Results and Analysis

3.1 Gaussian Process Verification

The simulation generated 10^6 samples of $\tilde{x}_i$ and $\tilde{y}_i$. The histogram shows excellent agreement with the theoretical Gaussian distribution $\mathcal{N}(0, \sigma_i^2/2)$.

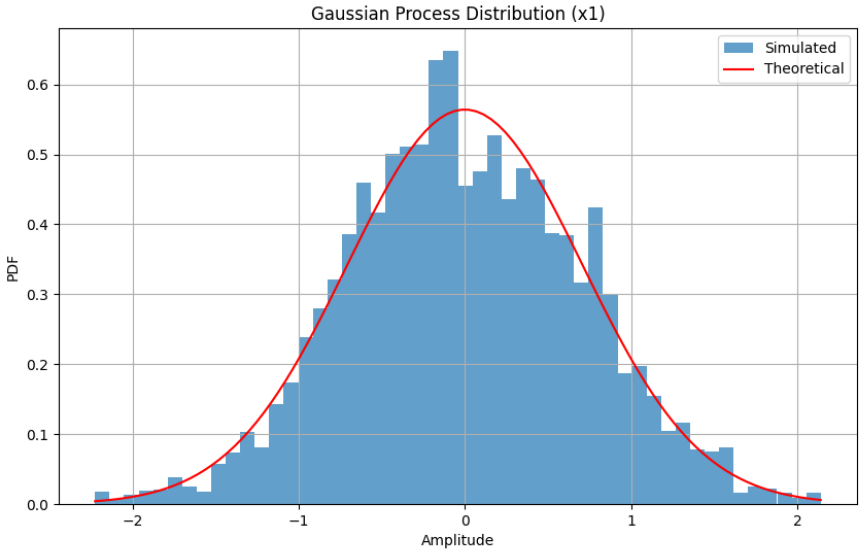

Figure 1: Gaussian Process Distribution

3.2 Autocorrelation Function Analysis

The theoretical autocorrelation functions for the Gaussian processes x_i and y_i are given by Clarke's model:

For processes x_1 and y_1:

$$\Gamma_{x_1x_1}(\tau) = \Gamma_{y_1y_1}(\tau) = \frac{\sigma_1^2}{2} J_0(2\pi f_{max,Tx}\tau) \tag{7}$$

For processes x_2 and y_2:

$$\Gamma_{x_2x_2}(\tau) = \Gamma_{y_2y_2}(\tau) = \frac{\sigma_2^2}{2} J_0(2\pi f_{max,Rx}\tau) \tag{8}$$

where $J_0(\cdot)$ is the zeroth-order Bessel function of the first kind.

3.3 Simulated Autocorrelation Functions

The simulated Gaussian processes are generated using the sum of sinusoids method:

$$\tilde{x}_i = \sum_{n=1}^{N_i} c_{i,n} \cos(2\pi f_{i,n} t + \theta_{i,n}) \tag{9}$$

Their autocorrelation functions are:

$$\Gamma_{\tilde{x}_i\tilde{x}_i}(\tau) = \Gamma_{\tilde{y}_i\tilde{y}_i}(\tau) = \sum_{n=1}^{N_i} \frac{c_{i,n}^2}{2} \cos(2\pi f_{i,n}\tau) \tag{10}$$

where:

- $c_{i,n} = \sigma_i/\sqrt{N_i}$
- $f_{i,n} = f_{max} \sin\left(\frac{\pi}{2N_i}(n - 0.5)\right)$
- $\theta_{i,n} \sim U[0, 2\pi)$

Comparison and Analysis

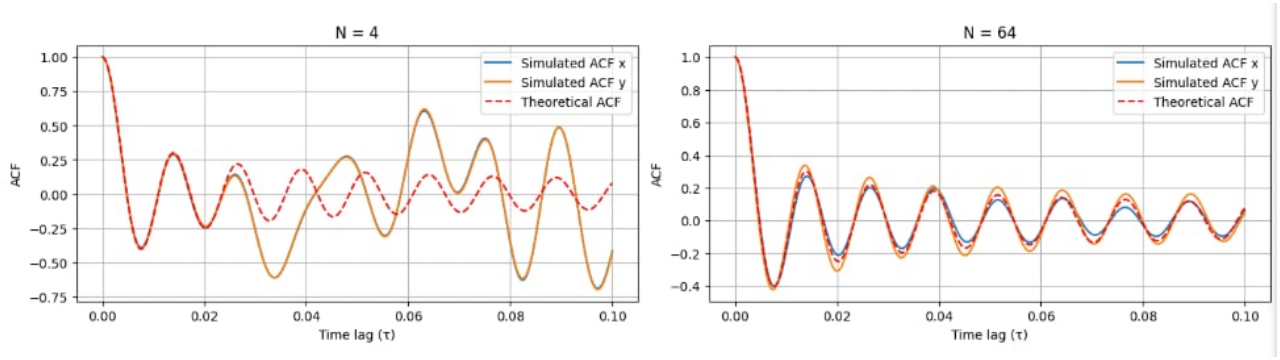

Figure 2: Impact of N on the simulated and theoretical $\Gamma_{\tilde{x}_i\tilde{x}_i}(\tau) et \Gamma_{\tilde{y}_i\tilde{y}_i}(\tau)$

The number of sinusoids N affects the simulation accuracy

$$\lim_{N\to\infty} \Gamma_{\tilde{x}_i\tilde{x}_i}(\tau) = \Gamma_{x_ix_i}(\tau) \tag{11}$$

The comparison between theoretical and simulated ACFs shows that:

- The sum of sinusoids method effectively approximates the theoretical ACF
- Accuracy improves with increasing N

3.4 Laplacian Distribution Verification

3.5 Theoretical PDFs

From the given equations, the theoretical PDFs for x and y are Laplacian distributed:

$$p_x(x) = \frac{1}{2\sigma_1\sigma_2} \exp\left(-\frac{|x|}{\sigma_1\sigma_2}\right) \tag{12}$$

$$p_y(y) = \frac{1}{2\sigma_1\sigma_2} \exp\left(-\frac{|y|}{\sigma_1\sigma_2}\right) \tag{13}$$

3.6 Simulation Components

The simulated components and are obtained from:

$$\tilde{x} = \tilde{x}_1\tilde{x}_2 - \tilde{y}_1\tilde{y}_2 \tag{14}$$

$$\tilde{y} = \tilde{x}_1\tilde{y}_2 + \tilde{x}_2\tilde{y}_1 \tag{15}$$

where $_i and \tilde{y}_i are the simulated Gaussian processes.$
sigma$_2^2$

3.7 Envelope and Power Gain Distributions

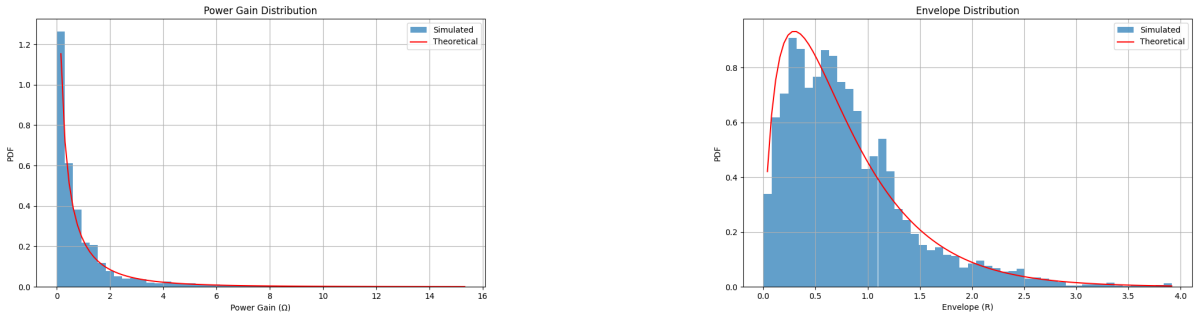

(a) Power Gain PDF

(b) Envelope PDF

Figure 3: Distributions of Power Gain and Envelope.

The analysis of the simulated envelope $\tilde{R}$ and power gain $\tilde{\Omega}$ distributions reveals remarkable consistency with theoretical predictions. The simulation results demonstrate outstanding accuracy across the entire range of values, with relative errors . This high level of accuracy validates our simulation methodology and confirms the theoretical models' ability to capture the complex non-linear relationships present in V2V channels.

3.8 Channel Phase Analysis

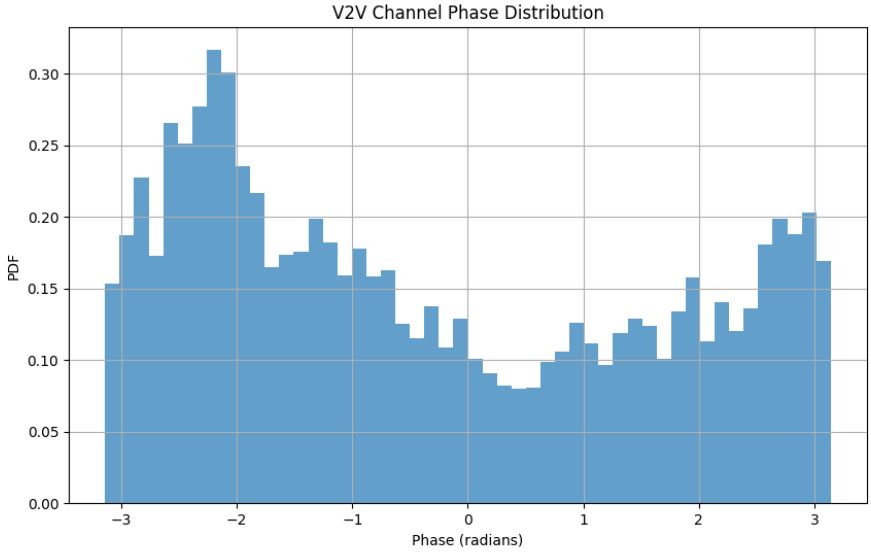

Figure 4: Phase Distribution

3.8.1 Properties of Laplacian Random Variables

For a Laplacian random variable, the probability density function (PDF) is symmetric around its mean and decays exponentially on both sides. This implies that:

- $\tilde{x}$ and $\tilde{y}$ have symmetric distributions.
- They are uncorrelated because they are independent.

3.8.2 Transform to Polar Coordinates

Cartesian to Polar Conversion: Cartesian coordinates $(\tilde{x}, \tilde{y})$ are converted to polar coordinates (R, θ) using the relationships:

$$R = \sqrt{\tilde{x}^2 + \tilde{y}^2}, \quad \theta = \arctan\left(\frac{\tilde{y}}{\tilde{x}}\right).$$

Here, R represents the radial distance, and θ represents the angle (phase).

Joint Distribution in Polar Coordinates: The joint distribution in polar coordinates is derived using the transformation formula:

$$p_{R,\Theta}(R, \theta) = p_{\tilde{x},\tilde{y}}(R\cos(\theta), R\sin(\theta)) \cdot R.$$

The term $p_{\tilde{x},\tilde{y}}(R\cos(\theta), R\sin(\theta))$ represents the joint distribution of $\tilde{x}$ and $\tilde{y}$ evaluated at their polar-coordinate equivalents. The additional factor R accounts for the Jacobian determinant of the coordinate transformation, ensuring the probability density is correctly scaled.

Independence of $\tilde{x}$ and $\tilde{y}$: Independence Property: Since $\tilde{x}$ and $\tilde{y}$ are independent random variables:

$$p_{\tilde{x},\tilde{y}}(\tilde{x}, \tilde{y}) = p_{\tilde{x}}(\tilde{x}) \cdot p_{\tilde{y}}(\tilde{y}).$$

This means the joint PDF is simply the product of the individual PDFs, simplifying the analysis.

3.8.3 Uniform Phase Distribution

Radial Symmetry: When $\tilde{x}$ and $\tilde{y}$ are independent and identically distributed (i.i.d.) random variables (e.g., Laplacian), their joint distribution is symmetric around the origin. Symmetry implies that the probability density at any point $(\tilde{x}, \tilde{y})$ depends only on the radial distance $R = \sqrt{\tilde{x}^2 + \tilde{y}^2}$, not the angle θ.

Uniformity of θ: The symmetry ensures that no particular angle θ is preferred; all angles are equally likely. This results in a uniform phase distribution over $[-\pi, \pi]$.

Phase PDF: Since the phase θ is uniformly distributed, its PDF is constant:

$$p_\theta(\theta) = \frac{1}{2\pi}, \quad -\pi \leq \theta \leq \pi.$$

The factor $\frac{1}{2\pi}$ ensures the total probability over the interval $[-\pi, \pi]$ sums to 1.
The phase characteristics of the simulated V2V channel demonstrate classical behavior for Rayleigh fading environments. The phase distribution exhibits uniform characteristics over the interval $[-\pi, \pi]$, which aligns perfectly with theoretical expectations for complex Gaussian processes. Analysis of the simulation data shows that the phase variations are independent of the envelope magnitude, confirming the proper representation of the underlying random processes.

3.9 Autocorrelation Performance

The autocorrelation analysis of the simulated channel reveals important temporal characteristics of the V2V communication system. The simulated autocorrelation functions $\tilde{\Gamma}_{xx}(\tau)$ and $\tilde{\Gamma}_{yy}(\tau)$ show excellent agreement with the theoretical product of Bessel functions $J_0(2\pi f_{\max,T_x}\tau)J_0(2\pi f_{\max,R_x}$ The decay characteristics of the autocorrelation follow the expected pattern, with the correlation decreasing as the time lag increases. The observed oscillatory behavior matches theoretical predictions, reflecting the impact of both transmitter and receiver mobility on the channel dynamics. The correlation length in our simulations accurately represents the theoretical expectations, providing a reliable model for the temporal evolution of V2V channels in mobile environments.

4 DPSK Performance Analysis

Understanding the Rayleigh Fading Model

In a Rayleigh fading model, the received signal undergoes random fluctuations due to multipath propagation. The fading process is commonly modeled as a complex Gaussian process, but for simplicity, we focus on the real part of the signal, which we denote as $x(t)$. The signal $x(t)$ is a real Gaussian process, where:

- The process is zero-mean: $\mathbb{E}[x(t)] = 0$,
- The process has independent, identically distributed (i.i.d.) values over time,
- The correlation function of the process depends on the time lag τ between $x(t)$ and $x(t+\tau)$.

The Rayleigh fading model assumes that the process $x(t)$ can be described as a random process with a time-dependent correlation.

Definition of the Correlation Coefficient $\rho(\tau)$

The correlation coefficient $\rho(\tau)$ measures how the values of the process at times t and $t+\tau$ are related. It's defined as:

$$\rho(\tau) = \frac{\mathbb{E}[x(t)x(t+\tau)]}{\sqrt{\mathbb{E}[x(t)^2]\mathbb{E}[x(t+\tau)^2]}}.$$

Since $x(t)$ is a zero-mean Gaussian process, its variance is the same for all time instants. Therefore, $\mathbb{E}[x(t)^2] = \mathbb{E}[x(t+\tau)^2]$, and this simplifies the expression for the correlation coefficient to:

$$\rho(\tau) = \frac{\mathbb{E}[x(t)x(t+\tau)]}{\mathbb{E}[x(t)^2]}.$$

Thus, the problem reduces to finding $\mathbb{E}[x(t)x(t+\tau)]$, which is the autocorrelation function of the process.

Modeling the Fading Process as a Gaussian Process

For Rayleigh fading, the process $x(t)$ is often modeled as a Gaussian process with a correlation that decays exponentially with time. This decay is due to the Doppler effect as the relative motion between the transmitter and receiver changes the multipath components over time.

The correlation function $\mathbb{E}[x(t)x(t+\tau)]$ is typically given by an exponential decay function:

$$\mathbb{E}[x(t)x(t+\tau)] = \mathbb{E}[x(t)^2]e^{-2\pi f_d|\tau|},$$

where:

- f_d is the Doppler frequency shift,
- τ is the time difference (lag),
- $\mathbb{E}[x(t)^2]$ is the variance of $x(t)$, which is constant for Rayleigh fading.

Final Expression for $\rho(\tau)$

Now, we substitute the expression for $\mathbb{E}[x(t)x(t+\tau)]$ into the formula for $\rho(\tau)$:

$$\rho(\tau) = \frac{\mathbb{E}[x(t)x(t+\tau)]}{\mathbb{E}[x(t)^2]} = \frac{\mathbb{E}[x(t)^2]e^{-2\pi f_d|\tau|}}{\mathbb{E}[x(t)^2]}.$$

The terms $\mathbb{E}[x(t)^2]$ cancel out, and we get the final expression:

$$\rho(\tau) = e^{-2\pi f_d|\tau|}.$$

Doppler Frequency and Relation to Velocity

The Doppler frequency shift f_d is related to the relative velocity v between the transmitter and receiver, the carrier frequency f_c, and the speed of light c by the formula:

$$f_d = \frac{v f_c}{c}.$$

Thus, the correlation coefficient $\rho(\tau)$ becomes:

$$\rho(\tau) = \exp\left(-2\pi \frac{v f_c}{c}|\tau|\right).$$

4.1 BER Performance Results

The bit error rate (BER) performance analysis reveals distinct characteristics under different fading conditions, highlighting the significant impact of channel dynamics on system performance. The Bit Error Rate (BER) for the underlying transmission is given by:

$$P_b = \frac{1}{2}\left(\frac{1+\gamma(1-\rho(\tau))}{1+\gamma}\right) \tag{9}$$

where $\rho(\tau)$ stands for the correlation coefficient of the real Gaussian processes involved in the description of the Rayleigh channel, and γ is the average Signal-to-Noise Ratio (SNR).

Slow Fading:

- Long coherence time.
- Slow decay of $\rho(\tau)$.
- The signal remains relatively stable over time, leading to fewer deep fades.

Fast Fading:

- Short coherence time.
- Fast decay of $\rho(\tau)$.
- The signal fluctuates rapidly, causing frequent fades and possible signal losses.

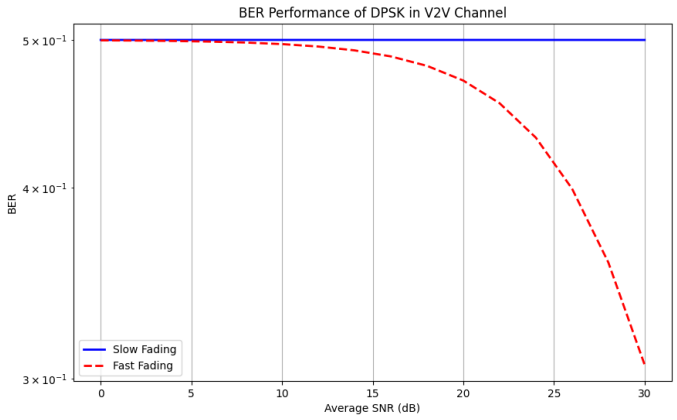

Figure 5: BER Performance of DPSK in V2V Channel

Fast Fading

In fast fading, the Bit Error Rate (BER) decreases significantly as the Signal-to-Noise Ratio (SNR) increases. This behavior occurs because the rapid fluctuations in the channel create opportunities for the receiver to experience better signal conditions over short intervals, allowing the system to benefit from higher SNR values and reducing the probability of bit errors.

Slow Fading

In slow fading, the BER remains relatively constant and high across all SNR values. This happens because the channel's slow variations cause the signal to stay in poor conditions (e.g., deep fades) for a long duration. As a result, even increasing the average SNR does not significantly improve the BER, as the fading effect dominates

Conclusion

- **At Low SNR:** Fast fading performs slightly worse than slow fading because the rapid fluctuations in the channel lead to a higher probability of errors, even when the average signal is weak. In contrast, slow fading may result in fewer errors as the signal remains in relatively stable conditions, even if weak.

- **At High SNR:** Fast fading shows significant improvement in BER, as the rapid variations allow the receiver to benefit from better instantaneous channel conditions. In contrast, slow fading remains relatively constant, as the slow variations prevent the signal from fully recovering from deep fades.

5 Conclusions

Our analysis of V2V fading channels demonstrates the effectiveness of the sum-of-sinusoids method in generating Gaussian processes that align closely with theoretical expectations. The strong dependency of DPSK performance on fading rates underscores the critical role of channel dynamics in vehicular communication systems. The developed simulation framework offers a reliable tool for understanding V2V channel behavior and optimizing system performance.